Scaling Intermittent Cross-Field Particle Flux to ITER

Ph. Ghendrih 1), P. Kaw 2), Y. Sarazin 1),
P. Beyer 3), S. Benkadda 3), G. Falchetto 1), X. Garbet 1), V. Grandgirard 1), M. Ottaviani 1)

1) Association Euratom-CEA, DRFC/DSM/CEA, CEA Cadarache,
13108 St Paul lez Durance, France
2) Institute for Plasma Research, Bhat, Gandhinagar, India
3) UMR 6633 PIIM CNRS-Université de Provence, 13397 Marseille, France

e-mail contact of main author : philippe.ghendrih@cea.fr

Abstract. Analysis of 2D interchange simulation in the Scrape-Off Layer indicates that intermittent outbursts of density dominate the transport process. It is possible to define density fronts, namely over-dense regions that follow ballistic trajectories in the SOL. The scaling law that relates the SOL width λ to the connection length $L_{//}$ is modified compared to the standard diffusive scaling. The simulations lead to $\lambda \propto L_{//}^{0.63}$. An analytical model based on the interplay between the average density and the over-dense fronts yields an exponent 5/8 (0.625). Such a departure from a diffusive scaling tends to yield a larger SOL width but, as a consequence, enhances the plasma-wall interaction in the main chamber and lowers the separatrix density at given particle source.

1. Introduction

Intermittent transport in the Scrape-Off Layer of magnetically confined fusion devices has been the matter of recent experimental and theoretical investigation [1-5]. There is a general trend to consider that cross-field transport of matter is governed by long range ballistic propagation. In particular, simulations of SOL density transport, where the external drive is a given particle source (flux driven) rather than a prescribed density gradient, are characterised by intermittent dynamics [1, 5]. In this case, the transport properties are described by Probability Distribution Functions of the particle flux and density with heavy tails [1, 3, 5]. These bear many similarities with experimental observations of SOL transport and fluctuations [3, 4]. The mechanism of ballistic propagation of density fronts in the SOL is a likely candidate to describe the flat SOL density profiles [6], and consequently large particle recycling on distant objects, that are reported in experiments. This renewed understanding of SOL transport is now considered in the extrapolation to ITER [7]. Of particular importance is the particle flux to the main chamber. With ballistic transport, it is expected that a larger particle flux will reach the wall, leading to enhanced recycling there. This would have several consequences, such a reduced divertor efficiency, since a fraction of particle recirculation would bypass the divertor, or enhanced tritium trapping on the large wall extent. Depending on the energy transferred by this ballistic transport, especially the ion energy, the power to the main chamber wall can exceed the limit of the present ITER design. It appears therefore of particular interest to investigate the scaling law of the intermittent cross-field transport with device size, typically the plasma major radius R.

In the present theoretical analysis of particle turbulent transport we characterise the particle outflux by the density e-folding length λ. For a diffusive transport as implemented in the 2D boundary plasma simulations for ITER, the standard scaling with device size is expected, $\lambda = (D_\perp L_{//} / c_s)^{1/2}$. $D_\perp$ is the particle diffusion coefficient, c_s the sound velocity stemming from the parallel loss at the sheath and $L_{//} = \pi q R$ is the parallel connection length proportional to the device major radius R, $\lambda \propto R^{1/2}$. For ballistic transport the expected scaling is $\lambda = L_{//} (V_\perp / c_s)$ where $V_\perp$ is the effective velocity of the transverse transport process. If the effective Mach number $M_\perp = V_\perp / c_s$ does not depend on R, the SOL width scaling is then

$\lambda \propto R^1$. Provided such a direct comparison of SOL width scaling is appropriate, one would expect an enhanced plasma-wall interaction in the main chamber compared to extrapolations based on present experiments and assuming a diffusive scaling. Given the importance of this issue, we address here the scaling law of the SOL width in terms of the connection length $L_{//} \propto qR$. Results are based on extensive simulations of 2D interchange turbulence in the SOL. The scaling law given by these simulations is backed by analytical models. Section 2 of this paper is dedicated to the turbulence model and to the definition of the fronts, Section 3 to the analytical investigation of the scaling laws of the SOL width, finally, in Section 4 the numerical results are reported.

2. SOL Dynamics with Interchange Turbulence

We use here a simplified model at constant electron temperature T_e in the cold ion limit of the interchange instability in the SOL, [8, 9]. In the flute approximation, one can reduce the dimension of the system to 2D, replacing the curvature operator by an effective mean curvature term g, and only taking into account the parallel transport via the sheath boundary loss terms at the end of the field lines, [8, 9]. The equations to be solved are then a particle balance equation, here for the electrons density normalised to a given arbitrary density n_0, $N = n / n_0$, and a charge conservation equation that yields an equation for the vorticity $\Delta_\perp \phi$ where ϕ is the electrostatic potential normalised by T_e / e. The two equations are then :

$$\begin{aligned} \left(\partial_t - D\nabla_\perp^2\right)N \quad + \left[\phi, N\right] \qquad\qquad &= -\sigma N e^{(\Lambda-\phi)} + S \\ \left(\partial_t - \nu\nabla_\perp^2\right)\nabla_\perp^2\phi + \left[\phi, \nabla_\perp^2\phi\right] + g\partial_y Log(N) &= \sigma\left(1 - e^{(\Lambda-\phi)}\right) \end{aligned} \qquad (1)$$

The diffusion coefficients D and ν are collisional particle diffusion and viscosity. The electric drift convection takes the standard form of Poisson brackets $[f,g] = \partial_x f \partial_y g - \partial_y f \partial_x g$, where $x = (r-a) / \rho_s$ is the minor radius normalised by the hybrid Larmor radius $\rho_s^2 = T_e / m_i$ and where $y = a\theta / \rho_s$, a is the plasma radius. The sheath loss terms depend on both the difference between the electric potential and the plasma floating potential Λ and on the sheath conductivity $\sigma = \rho_s / L_{//}$. At equilibrium, the particle source term S is then balanced by the end loss term (in the parallel direction). Typical values of the parameters used in the runs will be found in [5]. The numerical scan of device size is achieved with a scan on the control parameter σ. All simulation data, but the σ-scan, reported in this paper are obtained with the largest value of σ, that corresponds to a reduced connection length of order ~ 1 m. Very large simulation boxes are used, up to $2048\ \rho_s$ radially, that allow for two decades of density decrease in the radial direction.

The Probability Density Function of the radial particle flux at a given position allows one to describe the transport in terms of 3 fields. First, the average density field $\bar{n}$ (averaged over time and poloidal angle) that is characterised by the radial exponential decay λ. Second, a large number of small amplitude particle flux events are observed, both positive and negative. They balance out when computing the average transport. This random field will allow one to introduce a noise as third field in simplified descriptions. Finally, an exponential heavy tale of relatively rare events with large magnitude that accounts for most of the radial flux. These events are referred to as density fronts since they are related to over-dense regions of the plasma that move radially. In practise, the fronts are defined as the sets of points such that the density locally exceeds the average density by a given factor, here a factor 2. These points cluster in structures that represent about 10 % of the box size. These over-density are defined by $\tilde{n}(x,y,t)=[n(x,y,t)-\bar{n}(x,t)]H(n(x,y,t)-2\bar{n}(x,t))$, where the function H is the Heaviside function. At each time about 10 fronts can be identified and are characterised by a well defined boundary. This front selection criterion is depicted on Fig.(1), with a 2D plot of $n(x,y,t)/\bar{n}(x,t)$. A blow-up of a particular front is shown on the right hand side.

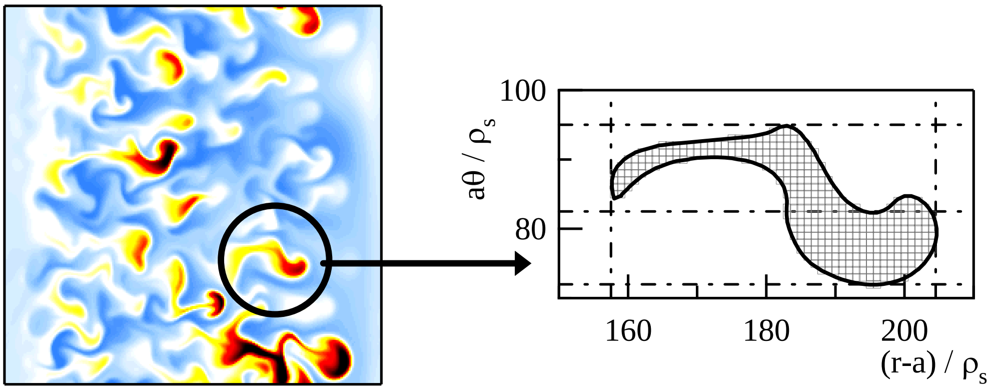

FIG. 1. Left 2D plot of the density divided by the average density profile, $n/\bar{n}$ in a 256 $\rho_s \times$ 256 ρ_s simulation box, right hand side, blow-up of a front defined by $n/\bar{n}>2$.

The simulations allow one to follow these structures in space and time so that they can be numbered and there statistical properties analysed. For example, one can compute their PDF of radial velocity and poloidal velocity (in terms of Mach numbers M_x and M_y since velocities are normalised to c_s), Fig.(2). In this analysis all values in x, y and t are used, on average for a given front $\langle M_y \rangle_t \sim 0$.

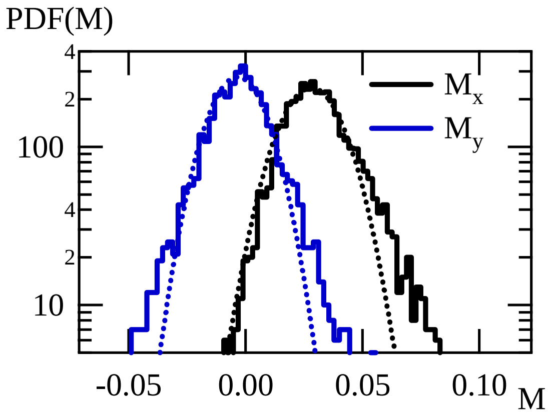

FIG. 2. Probability Distribution Function of the radial Mach number, M_x, and poloidal Mach number, M_y, of the fronts.

It is possible to use Eq. (1), together with multi-scale expansions in space and time, to generate a simplified set of equations for the average density field and the density fronts. In this approach, the average density field is determined by a balance between the parallel loss term $\sigma\bar{n}$ and a source term governed by the collisional diffusion of particles out of the front, typically $\tilde{n}/\tau_\perp$, where the time scale $\tau_\perp$ will depend on D and the characteristic scale of the front. The field $\tilde{n}$ is defined with two spatial dependences, one that characterises the geometry of the fronts, and we shall assume here that such a shape can be defined statistically and the magnitude of the front δn. We shall consider that the dynamics of the latter field is representative of the interaction between the density fronts and the average density as well as the build-up of the electrostatic dipole that governs the ballistic motion of the front.

In this approach, the source term S in Eq. (1) will lead to a source term for δn. The magnitude of the density front results from its generation mechanism in the region where the particle source S is located. In present simulations S is assumed uniform poloidally and with a gaussian radial localisation with characteristic extent $L_S = 8.5$ in units of ρ_s. In this early phase the scale of the front will be that of the most unstable mode of the linear growth. In a simplified approach, the front then propagates at a given velocity v_F. The characteristic duration of the front is τ_F. A key parameter is then the lag time between the fronts, τ_{lag}. All these quantities exhibit in fact a distribution. We will consider that they are independent so that only the average value is required in the analytical calculation of the scaling of the SOL width.

3. Analytical Scaling of the SOL Width

Let us first analyse the balance equation for the averaged density.

$$\partial_t \overline{n} \approx -\sigma \overline{n} + \frac{\delta n}{\tau_\perp} \frac{\Sigma_F}{\Sigma} \frac{\tau_F}{\tau_{lag}} \qquad (2)$$

As stated in Section 2, this equation is a balance between the parallel loss of density, with characteristic time $\tau_{//} = L_{//} / \sigma$, and the source due to particles diffusing out of the fronts. Two weight factors determine the magnitude of the source term due to the front, a time ratio and a surface ratio. The time ratio, τ_F / τ_{lag} between the time where this source is active τ_F. and the time lag τ_{lag}, is thus a measure of the effectiveness of the source in a time average. The surface ratio Σ_F / Σ is a ratio of the front cross-section, Σ_F, and the area where the front is the only source term Σ. This ratio is a measure of the effectiveness of the source term in a poloidal average. With these definitions, only the steady-state solution of Eq. (2) is relevant so that the balance between source and sinks relates the two functions of x, δn and $\overline{n}$.

$$\overline{n} \approx \frac{\delta n}{\sigma \tau_{lag}} \frac{\Sigma_F}{\Sigma} \frac{\tau_F}{\tau_\perp} \qquad (3)$$

Provided the average control parameter $(\tau_F \Sigma_F) / (\tau_\perp \tau_{lag} \Sigma)$ is not a function of x, one finds that the two functions δn and $\overline{n}$ must exhibit the same exponential decay, λ. Since the fronts propagate at a defined velocity, v_F, one can relate the front e-folding length to a balance between a convective radial transport with effective velocity $v_F\ \tau_F / \tau_{lag}$ and parallel loss term characterised by σ, so that :

$$\lambda = \frac{v_F \tau_F}{\sigma \tau_{lag}} \qquad (4)$$

The velocity of the front is derived from the vorticity equation in Eq. (1) with a time scale ordering to retain only the short time terms typically the variation of vorticity due to the front poloidal density gradient :

$$\partial_t \nabla_\perp^2 \phi \approx -\frac{g}{\overline{n}} \partial_y \tilde{n} \qquad (5)$$

This is a local effect so that the integration time is bounded by τ_F. The detailed shape of the front will determine the velocity distribution in the front, while the characteristic velocity will be related to δn.

$$v_F \approx g \frac{\delta n}{\overline{n}} \tau_F \qquad (6)$$

In order to relate the time lag τ_{lag} to the ratio $\delta n / \overline{n}$, one must analyse the source effect in the front generation as well as on the overall balance of particles. Regarding the global particle balance in the SOL, one considers an average over long times so that the contribution of the fronts in the parallel loss term is of order $\delta n\ \tau_F / \tau_{lag}$. That will be considered to be small with respect to $\overline{n}$. The loss term in the SOL is then given by $\sigma \overline{n}^* L_y \lambda$ with $\overline{n} = \overline{n}^* \exp(-x/\lambda)$. This term is balanced by the source term $S_0\, L_y\, L_S$ where S_0 is the magnitude of the source and L_S the source width. The scale L_y is the poloidal extent of the SOL. One thus finds that the magnitude of the mean density is proportional to the source term, as expected since Eq. (1) is autonomous with respect to *N*.

$$\overline{n}^* = \frac{S_0\, L_S}{\sigma \lambda} \qquad (7)$$

A last relation is obtained with the front generation in the source region. One then balances the source term integrated over the time τ_{lag}, $S_0\, L_S\, \tau_{lag}\, \Delta_F$ and the particle content of the front, $\delta n^*\, \Sigma_F$ (using $\delta n = \delta n^* \exp(-x/\lambda)$). In the first expression Δ_F is the poloidal wave length of the most unstable linear mode, it is used as the reference scale of the front. This yields the over-density :

$$\delta n^* = \frac{S_0\, L_S \tau_{lag} \Delta_F}{\Sigma_F} \qquad (8)$$

The time lag is thus related to the density ratio $\delta n / \overline{n} = \delta n^* / \overline{n}^*$ but independent of the magnitude and geometry of the source.

$$\sigma \tau_{lag} = \frac{\Sigma_F}{\lambda \Delta_F} \frac{\delta n}{\overline{n}} \qquad (9)$$

Combining Eqs.(4 & 9), one finds that the ratio $\delta n / \overline{n}$ is determined by the geometry of the front.

$$\frac{\delta n}{\overline{n}} = \frac{\Delta_F}{\Sigma_F} v_F \tau_F \qquad (10)$$

Given $\Sigma_F = v_F \tau_F\, \Delta_y$ where Δ_y is the characteristic poloidal extent of the fronts, one finds $\delta n / \overline{n} = \Delta_F / \Delta_y$. This is typically the ratio of the poloidal wave length in the linear phase Δ_F and of the poloidal extent of the front in the non-linear phase Δ_y. Provided that this ratio exhibits a weak dependence on the parameters in Eq. (1), one thus finds that $\delta n / \overline{n}$ is a constant that characterises the non-linear evolution of the front width. Eqs. (3 & 4) yields the density e-folding length.

$$\lambda = \left(\frac{g}{v_F \tau_F} \frac{\delta n}{\overline{n}} \right)^{1/2} \frac{\Sigma \tau_\perp}{\Delta_F} \qquad (11)$$

The area Σ is defined similarly to the area Σ_F, with a difference in poloidal extent since we have considered the front source to extend over Δ_F, $\Sigma = v_F \tau_F\, \Delta_F$, one then obtains the e-folding scale λ :

$$\lambda = v_F \tau_\perp \qquad where \quad v_F = \left(g \Delta_x \frac{\delta n}{\bar{n}} \right)^{1/2} \qquad (12)$$

In this expression, $\Delta_x = v_F \tau_F$ is the characteristic radial scale of the front. The e-folding length appears to stem from convective transport where the characteristic time is governed by a diffusion process, $\tau_\perp = A_\perp^2 \Delta_F^2 /$. $A_\perp$ is a scale ratio between the scale that governs the density diffusion process out of the front and the reference scale of the front, Δ_F. Similarly, let us define $A_x = \Delta_x / \Delta_F$. This leads to the scaling of the SOL width :

$$\lambda = \left(g A_x \frac{\delta n}{\bar{n}} \right)^{1/2} \frac{A_\perp^{\ 2}}{D} \Delta_F^{\ 5/2} \qquad (13)$$

Following the result of the linear analysis, one considers that the front width is determined by a balance between the two damping processes that govern the vorticity equation, namely the diffusion process of the form $-\nu \Delta W$, where W ($W = \Delta_\perp \varphi$)is the vorticity, and the sheath loss term of the order of σ, hence :

$$\Delta_F \approx \left(\frac{\nu}{\sigma} \right)^{1/4} \qquad (14)$$

With this expression one then finds that the SOL width λ scales like $\sigma^{-5/8}$ and therefore $L_{//}^{5/8}$ with $L_{//} = \pi q R$.

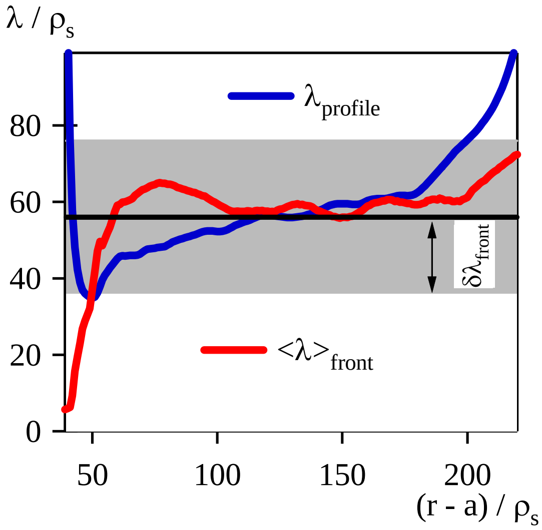

FIG. 3. Profile of the average density e-folding length $\lambda_{profile}$ in blue, and profile of the e-folding length of the magnitude of the density front (δn) $<\lambda_{front}>$ in red, the shaded area indicates the width of the distribution of λ_{front}

Another analytical investigation based on a simple scaling argument can be carried out. Let us assume that the SOL width is governed by a convective transport so that $\lambda_{ML} \sim V_{ML} / \bar{\sigma}$. The convective velocity is determined by $E \times B$ drift due to saturated turbulence, hence $V_{ML} \sim \phi_{ML}$. Based on a mixing length argument, the magnitude of the fluctuating field is proportional to the linear growth rate γ_L, so that $V_{ML} \sim \Delta_{ML}\, \gamma_L$. Well above the threshold, the linear growth rate scales like $(g / \lambda_{ML})^{1/2}$. This leads to the scaling $\lambda_{ML} \sim \Delta_{ML}\, (g / \lambda_{ML})^{1/2} / \sigma$. The $L_{//}$ scaling in this approach will then depend on the scaling of Δ_{ML}. If Δ_{ML} is taken constant, one finds that λ_{ML} scales like $L_{//}^{2/3}$. However, if one follows the prescription that Δ_{ML} be the wavelength of the most unstable mode in the linear analysis, then $\Delta_{ML} = \Delta_F$, see Eq. (14), so that λ_{ML} scales like $L_{//}^{5/6}$. Both results indicate that the scaling of the SOL width in terms of the connection length stands between a diffusive scaling $L_{//}^{1/2}$ and a ballistic scaling $L_{//}^{1}$.

4. Numerical Analysis of the SOL Width Scaling

Convective transport is used in both analytical calculations presented in Section 3. The evidence for such ballistic transport stems from the analysis of test particle transport as well as transport analysis of the profiles in terms of diffusion and convection transport. In both studies, one finds that the convective transport is dominant. A systematic statistical analysis has been performed. Based on these statistics, one finds that the motion of the fronts can be characterised by a velocity that varies slowly along the trajectory. A rather broad distribution of velocity is obtained, Fig.(2). This data indicates that one can describe the transport in terms of a given average convective velocity.

The statistical analysis also allows one to compare the e-folding length of the average density and that of the front magnitude, Fig.(3). For the density fronts, a distribution is obtained. The average value appears to support the identical e-folding length for both fields as introduced in Section 3. Finally, a scan of the connection length has been performed, Fig.(4). The simulation results are in line with a scaling $L_{//}^{0.63}$. The scaling based on front propagation thus appears to be in excellent agreement with this simulation result, $5/8 = 0.625$. However, the error bars do not allow one to discard the mixing length scaling that yields the exponent $2/3 = 0.67$. However, the simulation data clearly indicate that the characteristic poloidal scale of the electric potential exhibits a dependence in the parameter σ, following Eq. (14), a factor ~ 2 change is expected with the chosen scan of σ. Although the exact scaling has not be checked the observed change is in qualitative agreement with such a result. The more appropriate mixing length scaling then leads to the exponent $5/6 \sim 0.83$. The simulation data is sufficiently robust to discriminate between this value and the scaling indicated on Fig.(4).

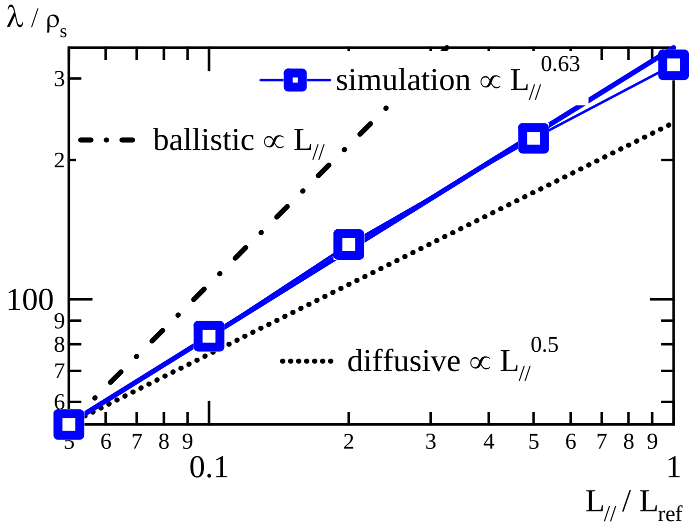

FIG. 4. Scaling of the density e-folding length λ versus the connection length $L_{//} = \pi qR$

The analytical calculation based on a two field description of transport, an average value and ballistic fronts, thus appears to yield the appropriate scaling of the SOL width. This is an important result, not only for the specific problem addressed in this paper, but more generally in order to incorporate the intermittent non-diffusive transport in the modelling effort. Indeed, compared to the present status of the modelling effort with 1D transport equations for the time averaged profile, one only requires one extra 1D equation for the dynamics of the magnitude of the fronts. This is far less demanding than running a global 3D fluid simulation in order to incorporate the appropriate transport in the modelling effort.

5. Discussion and Conclusion

In the analysis of the intermittent particle transport in the SOL, we have shown that the density field could be split into an average density profile and a set of over-dense fronts. The simulation of the plasma turbulence has allowed one to determine the statistical properties of the fronts, velocity distribution both radially and poloidally, Fig.(2). For $L_{//} \sim 1\ m$, The average radial propagation of the fronts is $0.03\ c_s$, with a rather broad quasi gaussian distribution. A similar statistical analysis is performed regarding the e-folding length of the magnitude of density of the fronts. Again a broad quasi-gaussian distribution is observed, the average value being very close to the e-folding length of the average density profile. These properties are used to analyse the scaling law of this e-folding length, hence the SOL width in terms of the connection length $L_{//}$. In this approach the average density results from the balance between the parallel loss term and a source term due to the collisional diffusion of particles out of the fronts. Since the average density and the magnitude of the density in the fronts are similar, the characteristic time scales of these processes must be comparable, $\tau_{//} \sim \tau_{\perp}$. The over-densities are generated in the source region, hence in the case of the SOL in the vicinity of the separatrix. The characteristic time lag between two fronts is such that $\tau_{lag} \sim \tau_{//} / 5$, while the characteristic lifetime of a front is $\tau_F \sim \tau_{//} /25$(with $L_{//} \sim 1\ m$). This ordering is an a posteriori justification for the separation of the density field into the average field and the fronts. This allows one to compute the scaling law of the SOL width in terms of the connection length, since $\tau_{//} \sim L_{//} / c_s$, and thus the major radius of the device. The exponent computed with the simulation data and the exponent derived analytically, are found to be in excellent agreement, ~0.63 with both methods. An alternative mixing length argument provides a similar value, 0.667.

These exponents are slightly bigger than that expected from a diffusive scaling law. They are smaller than would be found with a purely convective transport. When scaling up present experimental to ITER, one can then expect a larger SOL width than given by a diffusive scaling. This favourable trend is balanced by the fact that the separatrix density will be lower for a given particle source, see Eq.(7), and that the main chamber wall recycling will be enhanced.

References

[1] Y. Sarazin and Ph. Ghendrih Ph. 1998 *Phys. Plasmas* **5** 4214.
[2] J. A. Boedo et al, 2001, *Phys. Plasmas* **8** 2107.4826.
[3] G.Y. Antar, P. Devynck, X. Garbet, S.C. Luckhardt, Phys. of Plasmas, 8 (2001) 1612.
[4] S.I. Krasheninnikov, Phys. Letters A, 283 (2001) 368-370.
[5] Ph. Ghendrih et al. 2003, *Nucl. Fusion* **43** 1013.
[6] B. La Bombard. et al. 2001, *Phys. Plasmas* **8** 2107.
[7] B. Lipschultz B. 2004, private communication
[8] A.V. Nedospasov, Sov. J. Plasma Phys., 15 (1989) 659.
[9] X. Garbet, et al., Nucl. Fusion, 31 (1991) 967.